The EMBO Journal Vol.18 No.19 pp.5175–5186, 1999

Crystal structure and induction mechanism of AmiC–AmiR: a ligand-regulated transcription antitermination complex

Bernard P.O'Hara[1], Richard A.Norman[2], Paul T.C.Wan[1], S.Mark Roe[1,3], Tracey E.Barrett[1], Robert E.Drew and Laurence H.Pearl[1,3,4]

Department of Biochemistry and Molecular Biology, and [3]Joint UCL/Ludwig X-ray Crystallography Laboratory, University College London, Gower Street, London WC1E 6BT, UK

[1]Present address: Centre for Structural Biology, Institute of Cancer Research, Chester Beatty Laboratories, 237 Fulham Road, London SW3 6JB, UK
[2]Present address: Imperial Cancer Research Fund, 44 Lincoln's Inn Fields, London WC2A 3PX, UK

[4]Corresponding author

B.P.O'Hara and R.A.Norman contributed equally to this work

Inducible expression of the aliphatic amidase operon in *Pseudomonas aeruginosa* is controlled by an antitermination mechanism which allows production of the full-length transcript only in the presence of small-molecule inducers, such as acetamide. Ligand-regulated antitermination is provided by AmiC, the ligand-sensitive negative regulator, and AmiR, the RNA-binding positive regulator. Under non-inducing or repressing growth conditions, AmiC and AmiR form a complex in which the activity of AmiR is silenced. The crystal structure of the AmiC–AmiR complex identifies AmiR as a new and highly unusual member of the response-regulator family of bacterial signal transduction proteins, regulated by sequestration rather than phosphorylation. Comparison with the structure of free AmiC reveals the subtle mechanism of ligand-induced release of AmiR.

Keywords: amidase/response regulator/RNA-binding protein/signal transduction

Introduction

Inducible expression of the aliphatic amidase in *Pseudomonas aeruginosa* PAC1 is controlled by the *amiR* and *amiC* genes (Cousens *et al.*, 1987; Wilson and Drew, 1991), whose products constitute an amide-regulated transcription antitermination system (Drew and Lowe, 1989; Wilson *et al.*, 1993, 1996). In the absence of inducing amides, constitutive transcription of the amidase operon is prematurely terminated just downstream of the promoter (Wilson and Drew, 1995), at an inverted repeat sequence which forms a stable stem–loop structure in the nascent mRNA. In the presence of inducing amides, premature termination is prevented by AmiR, which interacts with the nascent mRNA upstream of the terminator and probably prevents formation of the stem–loop. In the absence of inducers, the antitermination activity of AmiR is inhibited by interaction with AmiC (Wilson *et al.*, 1993). AmiC is structurally homologous to the small-molecule binding proteins such as bacterial periplasmic receptors (Quiocho, 1991), and the ligand-binding domains of some transcriptional repressors such as LacI (Lewis *et al.*, 1996). AmiC binds amides at the interface of its N- and C-terminal domains (Pearl *et al.*, 1994), and is responsible for the amide sensitivity and specificity of the system.

The biochemical mechanism by which the AmiC–AmiR system is induced by the presence of amides has been unclear. Recently, however, we have succeeded in purifying a stable AmiC–AmiR complex from cells grown in the presence of the co-repressor butyramide (R.A.Norman, B.P.O'Hara, L.H.Pearl and R.E.Drew, manuscript in preparation). Addition of an inducing amide disrupts this purified complex *in vitro* and enables sequence-specific binding of AmiR to RNAs containing the sequences upstream of and including the inverted repeat (R.A.Norman, B.P.O'Hara, L.H.Pearl and R.E.Drew, manuscript in preparation). These data suggest that the AmiC–AmiR complex is the silenced state of AmiR, which is then released by conformational changes in AmiC on amide binding. We have now determined the crystal structure of the AmiC–AmiR complex in the presence of butyramide, revealing the structural basis for the silencing of AmiR activity by AmiC and revealing the molecular mechanism for inducer-mediated disruption of the AmiC–AmiR complex. The structure of AmiR identifies it as a member of the large family of two-domain response regulators that mediate signal transduction in bacteria. However, unlike these systems, AmiR is an intimate dimer with a coiled-coil interface; it functions by binding RNA (Wilson *et al.*, 1996), and is controlled by ligand-regulated sequestration rather than phosphorylation. Structural homologues of AmiR, at least one of which shares a common function in positive regulation of operon expression, suggest that AmiR is the first structurally defined representative of a new family of RNA-binding response regulators. The mechanism for control of AmiR antitermination activity by sequestration in a ligand-disruptable silencing complex would appear so far to be unique.

Results and discussion

AmiR structure

AmiR is present in the crystals as an intimate dimer of the 197 residue AmiR monomer (Figure 1) complexed with AmiC (see below). AmiR itself consists of an N-terminal doubly wound α-β-α sandwich domain (2–128) constructed around five parallel β-strands with *b-a-c-d-e* topology. The C-terminus of this domain is extended into a substantial α-helix 55 residues long, which participates in a parallel coiled-coil interaction over 30 residues (129–160) with the equivalent helix of the other

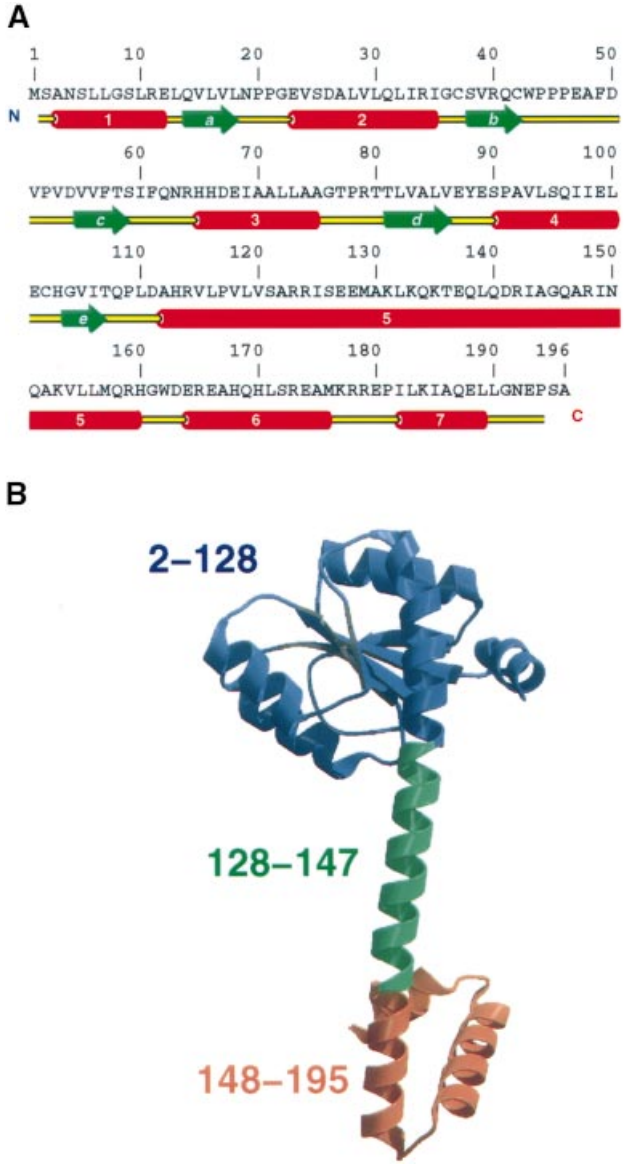

Fig. 1. AmiR secondary structure and domains. (**A**) Secondary structure of AmiR mapped on to the amino acid sequence (Swissprot Entry AMIR_PSEAE, but with residue 64 corrected to arginine). (**B**) Domain structure of AmiR monomer. N-terminal globular domain (blue), central coiled-coil region (green) and C-terminal helical domain (red).

monomer. The C-terminus of this helix (residues 145–159) participates in a three-helix bundle involving the remainder of the peptide chain (residues 160–195). No electron density is observable for the N-terminal methionine, which has presumably been removed, nor for a few residues at the C-terminus, which extend out from the C-terminal helical bundle.

The dimer interface between the AmiR monomers is primarily hydrophobic, and is dominated by the coiled-coil interactions along the full length of the long helices involving residues 129–160 from each chain (Figure 2). Additional interactions involve the helix from 91 to 101, which packs against the beginning of the N-terminal helix (2–10) and the initial segment of the large helix (113–123) on the other monomer. Formation of the dimer buries ~1350 Å^2 of molecular surface per monomer. The monomers are not symmetrically equivalent, the major difference resulting from a small kink in the coiled-coil segment at Gly145. The coiled-coil interface is formed by the mutual hydrophobic packing of the side chains of residues Ile125, Met129, Leu132, Leu139 and Ile143, and a buried hydrogen bonding interaction between the side-chain hydroxyls of Thr136 from each chain.

AmiR is a response regulator

Comparison of AmiR with known structures revealed a significant but quite unexpected similarity between the N-terminal α-β-α sandwich domain (2–128) of AmiR and the response-regulator 'receiver' domain of bacterial two-component signal transduction systems (Parkinson, 1993) (Figure 3A). These domains occur in a wide variety of bacterial signalling systems, either as the isolated domain in the chemotaxis regulator CheY (Stock *et al.*, 1989; Volz and Matsumura, 1991) and the sporulation regulator Spo0F (Madhusudan *et al.*, 1996), or more commonly as an N-terminal domain prepended to one or more C-terminal 'output' domains (Hakenbeck and Stock, 1996). Unlike the receiver domains, the C-terminal domains have no common structure and provide output functions as diverse as DNA binding (Baikalov *et al.*, 1996; Martinez-Hackert and Stock, 1997) and methylester hydrolysis (Djordjevic *et al.*, 1998). The presence in AmiR of an N-terminal 'receiver' domain, coupled to a C-terminal domain, strongly suggests that AmiR is, at least structurally, a new member of the extensive family of bacterial response regulators. However, there are several features of AmiR that are quite distinctive, both structurally and mechanistically.

In the well-characterized and ubiquitous signal transduction systems regulating bacterial chemotaxis, osmoregulation and nitrogen assimilation (reviewed in Parkinson, 1993; Hakenbeck and Stock, 1996), the receiver domain in the response-regulator component is phosphorylated (and often dephosphorylated) by histidine kinases (Hess *et al.*, 1988) which act as the 'sensor' for the relevant stimulus. The functional state of the response regulator depends on the state of phosphorylation of the receiver domain. Thus, the single domain chemotaxis response regulator CheY only binds to the flagellar motor, whose direction of rotation is thereby inverted, in the phosphorylated state (Barak and Eisenbach, 1992; Roman *et al.*, 1992). In multidomain response regulators such as the DNA-binding nitrate/nitrite utilization regulator NarL (Baikalov *et al.*, 1996) or the chemotaxis methylesterase CheB (Djordjevic *et al.*, 1998), phosphorylation is believed to elicit a change in the relative conformation of the receiver and output domains. This unmasks the functional surface of the output domain which is occluded by the receiver domain in the dephosphorylated state. Phosphorylation in all of these systems is achieved by a Mg^{2+}-dependent phosphoryl transfer from a phosphohistidine in the histidine kinase sensor component, to an aspartic acid at the exposed C-terminus of the central β-strand *c* in the receiver domain of the response regulator (Sanders *et al.*, 1989, 1992). In addition to the phosphoryl acceptor, two aspartyl (or sometimes glutamyl) residues at the C-terminus of β-strand *a* are implicated in Mg^{2+} binding and catalysis of the phosphoryl-transfer reaction (Stock *et al.*, 1993). A threonine or serine, and a lysine

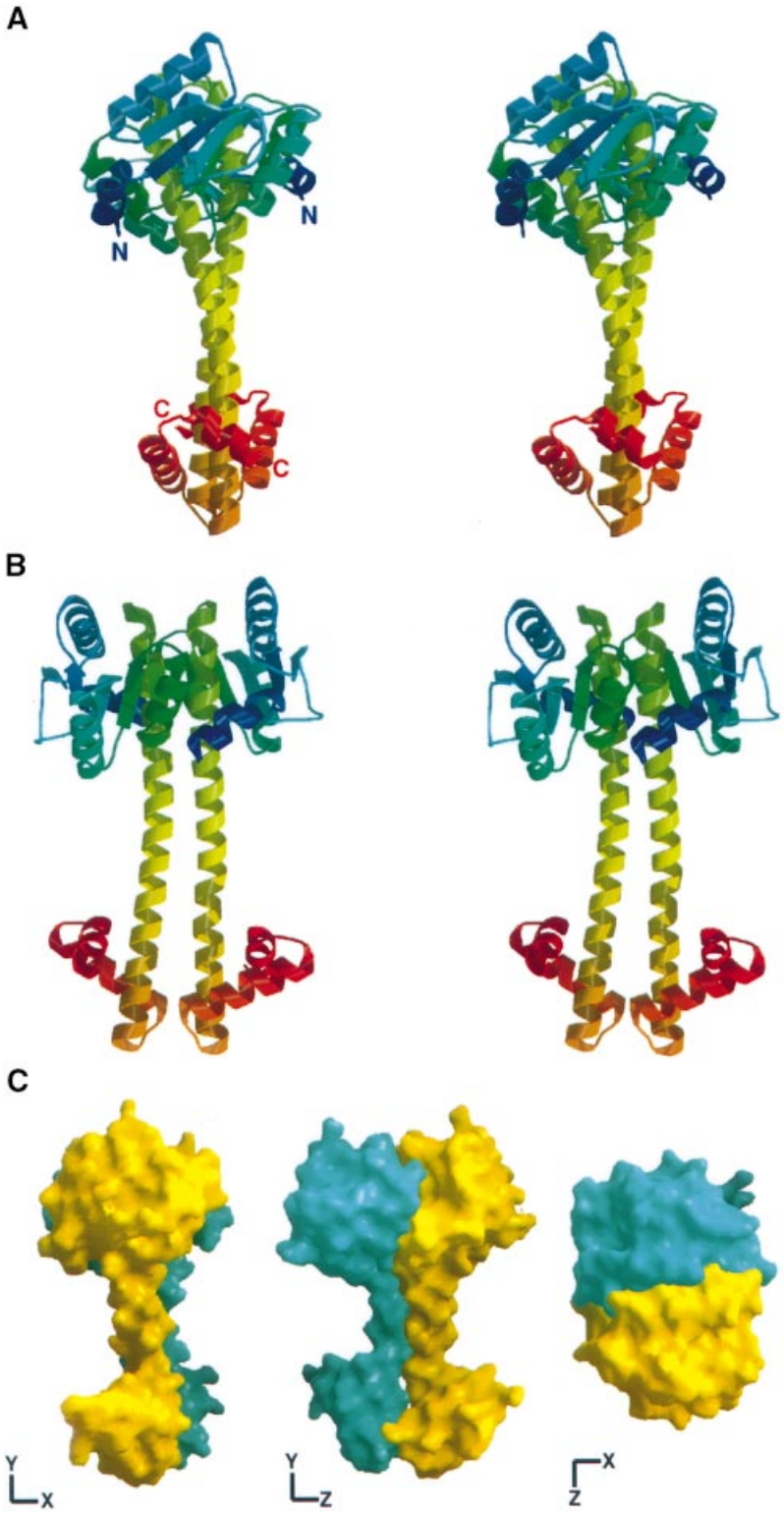

Fig. 2. AmiR dimer. (**A**) Stereo-pair showing the overall structure of the AmiR dimer, coloured blue (N-terminus) to red (C-terminus). (**B**) View perpendicular to (A). (**C**) Molecular surfaces of protomers in the AmiR dimer, viewed perpendicular (left and central) and parallel to (right) the ~2-fold axis of the dimer.

at the C-termini of β-strands *d* and *e*, respectively, are implicated in post-phosphorylation signalling (Lukat *et al.*, 1991; Ganguli *et al.*, 1995). Although regulation by phosphorylation has been demonstrated directly only for a few systems, the residues involved are very highly conserved in several hundred response regulators in bacteria (Stock *et al.*, 1990; Volz, 1993) and some eukaryotes (Imamura *et al.*, 1998; Thomason *et al.*, 1998). In AmiR, however, despite the high structural homology of its N-terminus to receiver domains, none of these residues are conserved. In a structural alignment of AmiR and CheY (Figure 3B), the residue corresponding to the

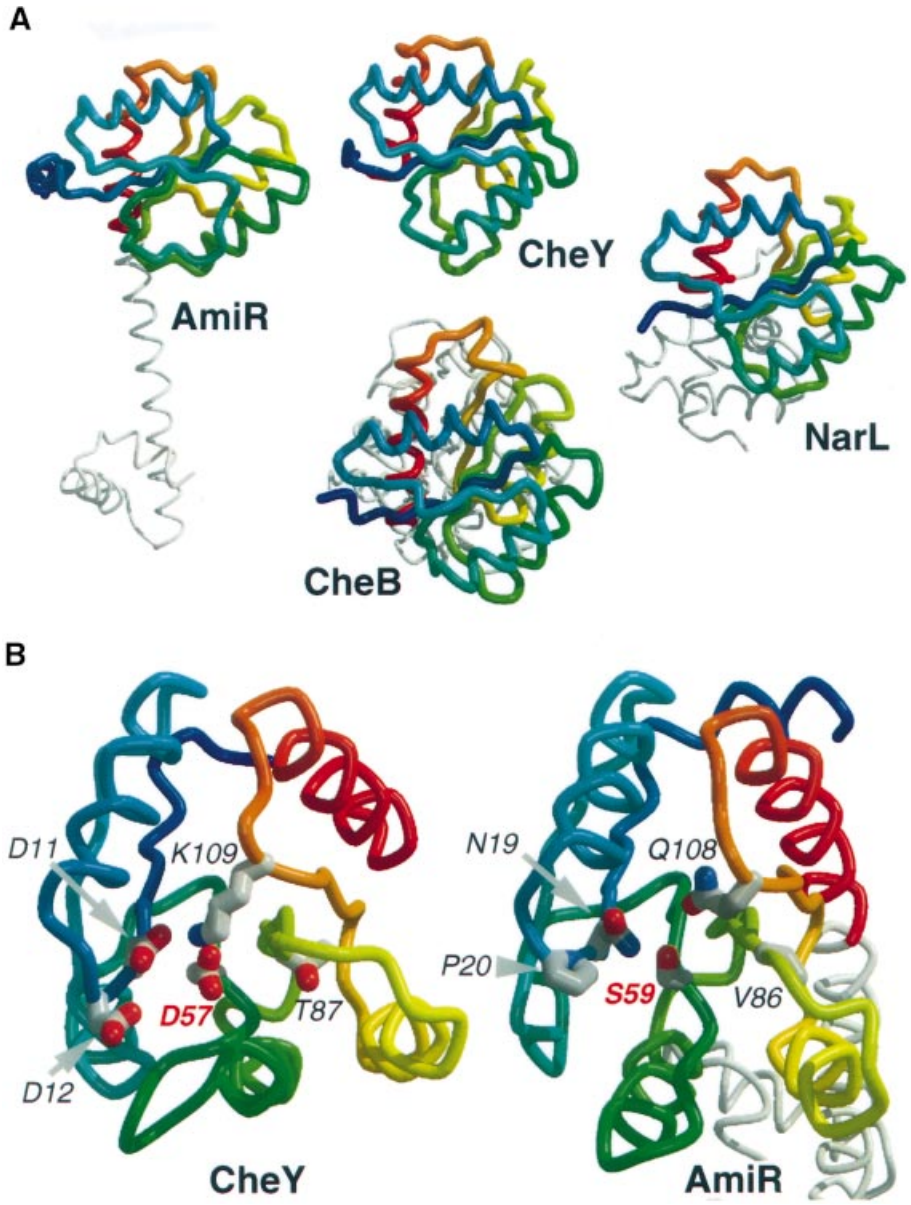

Fig. 3. Structural homology of AmiR to response regulators. (**A**) Comparison of AmiR with structures of bacterial response regulators CheY [Protein databank (PDB) code: 2CHF], CheB (PDB code: 1A2O) and NarL (PDB code: 1RNL). The 'receiver' domain common to these proteins is coloured blue to red (N-terminus to C-terminus) and the structurally disparate effector domains of AmiR, CheB and NarL are shown in grey. (**B**) Residues involved in phosphoryl transfer in CheY (left) and conserved in virtually all known response-regulator 'receiver' domains, but not in AmiR (right).

conserved phosphoryl acceptor Asp57 in CheY is Ser59 in AmiR; the aspartates at 12 and 13 in CheY are replaced by Asn19 and Pro20; Thr87 in CheY becomes Val86 in AmiR and Lys109 in CheY becomes Gln108 in AmiR. The lack of the requisite residues for phosphoryl transfer would suggest that AmiR is the first characterized member of the extensive response-regulator family, in whose function phosphorylation plays no role.

In the classic two-domain response regulators, the N-terminal receiver domain provides phosphorylation-sensitive regulation, while the C-terminal domain(s) encapsulates the regulated output function(s), the nature of which is specific to the individual system. Transcription factor response regulators such as NarL (Baikalov *et al.*, 1996), which control gene expression by direct interaction with DNA, do so via a five-helix C-terminal output domain which presents a helix–turn–helix reading-head (Harrison, 1991) into the major groove. Superficially, the coiled-coil and three-helix bundle that form the C-terminal part of AmiR appear radically different to the compact NarL DNA-binding domain. However, the last three helices in AmiR are very similar in their lengths and hydropathy profiles to those of NarL and its homologues, and are arranged in a very similar topology, suggesting an evolutionary relationship. The long helix connecting these terminal three helices to the receiver domain in AmiR could correspond to the third helix of the NarL DNA-binding domain, extended by concatenation with the first two helices of that domain, and with the hydrophobic residues thus exposed being reburied in the coiled-coil interface of the AmiR dimer.

Regardless of any evolutionary relationship to the DNA-binding NarL family of response regulators, previous studies (Wilson *et al.*, 1993, 1996) have shown clearly

Table I. Antitermination activity of AmiR mutants

Amide[a]	XL Int[b]	XL Int pBSK[c]	XL Int pBSKCR (WT)[d]	XL Int pBSKCR (Δ162–195)[d]	XL Int pBSKCR (Δ179–195)[d]	XL Int pBSKCR (Y88A)[d]
None	0.37	0.31	1.09	0.29	0.43	1.05
Acetamide	0.47	0.45	8.26	0.31	0.36	6.74
Butyramide	0.47	0.44	1.18	0.26	0.34	2.92

[a]Activities (in Miller units) were measured for bacterial cells grown under identical conditions with no amide, 34 mM acetamide or 23 mM butyramide present in the medium. Mutation of Tyr88(R), which lies at the AmiC–AmiR interface, converts butyramide into a weak inducer, but does not impair the antitermination activity of AmiR. Truncation of the C-terminal helices of AmiR (Δ179–195 and Δ162–195) completely abolishes transcription antitermination activity.
[b]XL Int: *E.coli* (XL1-Blue) with integrated *amiE*-leader–*lacZ* reporter gene (–ve control).
[c]XL Int pBSK: as XL Int but harbouring empty cloning vector pBSK (–ve control).
[d]XL Int pBSKCR: as XL Int but harbouring pBSK with cloned *amiCR* genes, with either wild-type (WT) *amiR* (+ve control), or with truncation (Δ162–195 or Δ179–195) or missense (Y88A) mutations in *amiR*.

that AmiR is an RNA-binding transcription antitermination protein, and by analogy with the classic response regulators, this 'output' activity should reside in the C-terminal regions. Consistent with this, truncation mutants of AmiR lacking either the last helix (Δ179–195) or the last two helices (Δ162–195) lack transcription antitermination activity (Table I), but are nonetheless stable soluble proteins (data not shown). Although the C-terminal helices of AmiR appear to be essential for its transcription antitermination activity, helix–turn–helix reading-heads like those in NarL (Baikalov *et al.*, 1996) or OmpR (Martinez-Hackert and Stock, 1997) are adapted to sequence-specific binding in the major groove of double-stranded B-form DNA. It is not at all obvious how such a structure might function in a protein whose role is to prevent the formation of a termination stem–loop structure, by binding single-stranded RNA.

Database searches with the AmiR sequence identify three homologues with sequence identities in the 20–30% range: an ORF in *Mycobacterium tuberculosis*, an ORF downstream of the *glnA* gene in *Clostridium acetobutylicum* and the *nasT* gene of *Azotobacter vinelandii*. Although the *M.tuberculosis* and *C.acetobutylicum* ORFs are of unknown function, NasT, like AmiR, is a positive regulator of gene expression (Gutierrez *et al.*, 1995). All three proteins share the pattern of hydrophobic residues that forms the coiled-coil interface in AmiR, suggesting that they are also likely to be dimers.

Structure of the AmiC–AmiR complex

The AmiC–AmiR complex crystallizes with an AmiR dimer and two AmiC monomers in the asymmetric unit (Figure 4A and B). Size-exclusion chromatography of the complex purified from *P.aeruginosa* (Wilson *et al.*, 1996; R.A.Norman, B.P.O'Hara, L.H.Pearl and R.E.Drew, manuscript in preparation) indicates a relative molecular mass of 130 kDa, consistent with a composition of 2 × AmiC (relative molecular mass 42.8 kDa) + 2 × AmiR (relative molecular mass 21.8 kDa), suggesting that the asymmetric unit represents the complex as it exists in solution. The crystal lattice is primarily stabilized by interactions between AmiC molecules in different AmiC–AmiR complexes, with only a few lattice interactions involving side chains on one helix of the AmiR dimer coiled coil. The lack of significant lattice interactions involving the C-terminal regions of AmiR is consistent with the higher temperature factors and weaker electron density observed for this part of the complex, while the asymmetry of those interactions that do exist appears to promote the bending of the coiled coil.

The two AmiC molecules in the complex bind to the 'top' surface formed by the two N-terminal AmiR domains, interacting simultaneously with both molecules in the AmiR dimer, and with each AmiC–AmiR interaction burying ~1520 Å^2 of molecular surface, on complex formation. The two AmiC molecules themselves make only a single side chain to side chain interaction, and effectively bind to the AmiR dimer as independent molecules. Despite the deviation from perfect 2-fold symmetry towards the C-terminus of the AmiR molecules, the two AmiC molecules in the complex make essentially identical interactions with the AmiR dimer. The major interaction between AmiC and AmiR involves a contiguous segment of polypeptide chain residues 88–93 of AmiR, which comprises the loop connecting the C-terminus of β-strand *d* to the N-terminus of α-helix 4 (Figure 4C). This AmiR loop binds across the fissure dividing the N- and C-domains of AmiC, making a series of complementary and interlinked interactions with surface residues from both AmiC domains. At the N-terminus of the α-helix 4 of AmiR, the exposed peptide nitrogens of Ala92(R) and Val93(R), and the side-chain hydroxyl of Ser90(R), are simultaneously hydrogen bonded to the side chain of Glu155(C) from the C-domain of AmiC. The γ and δ side-chain methylenes of Pro91(R) are then packed in van der Waals contact against the face of the side-chain ring of Phe111(C) from the N-domain of AmiC, while the side chain of His158(C) from the C-domain of AmiC stacks against the side chain of Ala92(R), and the plane of the peptide bond connecting it to Pro91(R). Further back along the loop, the side chain of Glu 89(R) hydrogen bonds to the phenolic hydroxyl of Tyr366(C) from the C-domain of AmiC, and the side chain of Tyr88(R) packs between the side chains of Ile151(C) from the C-domain of AmiC, and the hydrophobic segment of the side chain of Lys89(C) from the N-domain.

The same AmiC molecule makes a more diffuse set of interactions with the other AmiR molecule in the dimer, but again involving interactions from both AmiC domains (Figure 4B). The side-chain amide of Gln31(R) makes a hydrogen bond with the side chain of Tyr366(C) from the C-domain of AmiC, which is also involved in contacts with the other AmiR in the dimer. Asp364(C), also from the C-domain of AmiC, receives bidentate hydrogen bonds

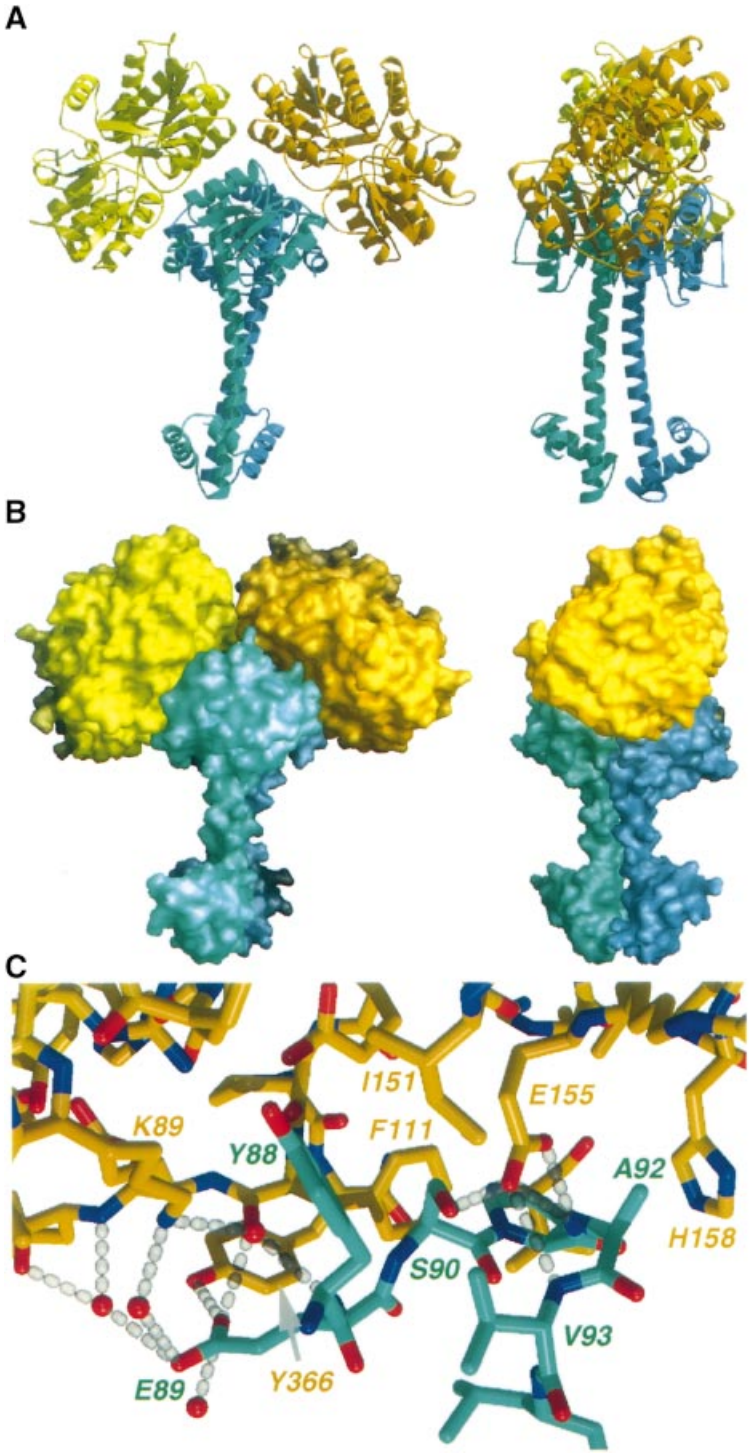

Fig. 4. Structure of the AmiC–AmiR complex. (**A** and **B**) Arrangement of AmiC (yellow/gold) and AmiR (blue/green) molecules in the AmiC–AmiR complex. Each AmiC molecule participates in an extensive interface with the N-terminal 'receiver' domains from both AmiR molecules, but the two AmiC molecules make no direct contact with each other. (**C**) Detail of part of the AmiC–AmiR interface showing the interactions involving the AmiR sequence from Y88–V93. Hydrogen bonds are shown as broken white rods and solvent molecules as red spheres.

from the guanidinium head-group of Arg11(R). His113(R) makes a hydrogen bond to the side chain of Glu96(C) from the N-domain of AmiC, while the guanidinium head-group of Arg34(R) is simultaneously hydrogen bonded to the peptide carbonyl of Gln332(C), and stacked in a π–π interaction with the phenol side chain of Tyr113(C), both from the N-domain. In addition to the direct interactions between the AmiR dimer and the two AmiC monomers, a substantial number of well-ordered solvent molecules are trapped at the AmiC–AmiR interfaces.

The molecular mechanism for amide induction of the amidase operon

The regulatory apparatus of the amidase operon can exist in three states, dependent on growth conditions (R.A.Norman, B.P.O'Hara, L.H.Pearl and R.E.Drew,

manuscript in preparation). In the non-induced state, a ligand-free AmiC–AmiR complex exists, in which the transcription antitermination activity of AmiR is silenced by AmiC. The presence of an amide inducer such as acetamide switches the system to the induced state in which AmiR facilitates full-length transcription of the operon. A third state, in which the system is repressed and resistant to induction, results from the presence of butyramide, which acts as a co-repressor, stabilizing the AmiC–AmiR complex. Sensitivity to amides requires AmiC, so that in the absence of the *amiC* gene, AmiR is constitutively active and unaffected by the presence or absence of inducing or co-repressing amides. As amide-triggered induction of heterologous genes can be fully reconstituted in *Escherichia coli* by the *amiCR* genes and the 5′-untranslated region of the amidase operon, the switch from uninduced (or repressed) to induced must therefore involve a change of state of the AmiC protein in the presence of an inducer.

By analogy with the periplasmic binding proteins (Quiocho, 1991) to which AmiC is homologous (Wilson *et al.*, 1993; Pearl *et al.*, 1994), we had previously suggested that AmiC possesses two conformational states: a 'closed' conformation stabilized by binding of an inducing ligand such as acetamide at the interface of the N- and C-domains, and an 'open' state in either the absence of inducer or the presence of butyramide, in which AmiC inhibits the transcription antitermination function of AmiR by direct protein–protein interaction (Wilson *et al.*, 1993). The previously determined structure of the complex between AmiC and acetamide (Pearl *et al.*, 1994) corresponds to the 'closed' state, and the AmiC–AmiR complex described here corresponds to the 'open' state. Thus, we are now able to understand the molecular basis of the acetamide-triggered conformational switch that regulates the activity of AmiR, and thereby the expression of the amidase operon.

The major difference between the closed structure of AmiC with bound acetamide (the induced state) and the open structure of AmiC in the AmiC–AmiR–butyramide complex (uninduced/repressed state), is in the relative orientation of the N- and C-domains (Figure 5A). In the closed conformation observed in the acetamide complex, the opposing walls of the N- and C-terminal domain are in direct contact. The aliphatic carbon chain of acetamide in the AmiC–acetamide complex structure binds in a hydrophobic pocket delimited by the side chains of Pro107 and Tyr83 from the N-domain, and Tyr152, Val206 and Thr233 from the C-domain (Figure 5B). The size of this pocket formed at the interface of the domains in the 'closed' conformation of AmiC determines the inducer specificity of the system. Thus, the pocket comfortably accommodates the aliphatic carbon chains of the inducers acetamide (1-carbon chain), propionamide or lactamide (2-carbon chain). Butyramide, whose longer 3-carbon chain cannot be readily accommodated, binds to AmiC with at least 100-fold lower affinity than acetamide (Wilson *et al.*, 1993), and is a co-repressor of the wild-type operon (Brammar *et al.*, 1967).

In the uninduced AmiC–AmiR complex, AmiC has a more open conformation in which the N- and C-domains become separated by a small relative hinge motion. Opening of the domain interface allows the ingress of a layer of water molecules between the opposing faces of the domains, and significantly increases the size of the amide-binding pocket. In particular, the side chain of Thr233, which caps the binding site for the amide aliphatic chain, moves over 2 Å from its position in the 'closed' conformation, allowing the binding of butyramide (Figure 5C). The presence of butyramide throughout expression and purification stabilizes the AmiC–AmiR complex against gratuitous disruption by acetamide, which is present in the growth medium (Pearl *et al.*, 1994). Although butyramide competes with acetamide for binding to free AmiC (Wilson *et al.*, 1993), it has a much lower binding affinity. The co-repression activity of butyramide can now be understood in terms of competition for the larger amide-binding pocket present in AmiC in the non-induced AmiC–AmiR complex, rather than for the smaller pocket of free AmiC. Although butyramide stabilizes the AmiC–AmiR complex in the presence of acetamide, it is not required for formation of the complex, and can be removed by dialysis after purification, without disruption of the complex (R.A.Norman, B.P.O'Hara, L.H.Pearl and R.E.Drew, manuscript in preparation).

In the AmiC–AmiR complex, AmiC surface residues from either side of the interdomain fissure make a set of highly complementary interactions with the 'top' face of the AmiR dimer. The formation of these interactions is absolutely dependent on the open conformation, so that superimposition of either domain of closed AmiC on to the corresponding domain in the AmiC–AmiR complex results in substantial steric clashes between the other domain and AmiR. The closed conformation of AmiC is thus incompatible with maintenance of the complementary AmiC–AmiR interface, and closure of AmiC on acetamide binding would inevitably disrupt the AmiC–AmiR complex. As the AmiC–AmiR complex is stable in the absence of acetamide, the switch to the induced state in the presence of acetamide therefore depends on a decrease in free energy on formation of the AmiC–acetamide complex exceeding any increase in free energy resulting from disruption of the AmiC–AmiR complex.

In binding acetamide, AmiC makes all possible hydrogen bonding interactions with the amide head-group, and van der Waals interactions with the aliphatic chain (Pearl *et al.*, 1994). Nonetheless, acetamide is a small molecule, and at first sight the interactions gained by AmiC binding acetamide do not obviously outweigh the number of interactions lost between the AmiC and AmiR proteins on disruption of their complex. However, a large number of solvent molecules are immobilized in the AmiC–AmiR complex, both at the interface between AmiC and AmiR molecules (~24 in the C_2R_2 dimer), and between the N- and C-domains of the AmiC molecules in their open AmiR-bound conformation (approximately five per AmiC). Release of these ordered molecules back to bulk solvent on disruption of the AmiC–AmiR complex will be very entropically favourable, and may well be a significant factor in the free energy balance that favours the disruption of AmiC–AmiR in the presence of acetamide.

The switch is clearly very subtle, and the energy difference between the induced and non-induced states is likely to be quite small. In the wild-type system, acetamide (1-carbon chain) is an effective inducer, whereas formamide (0-carbon chain) is not, suggesting that the binding

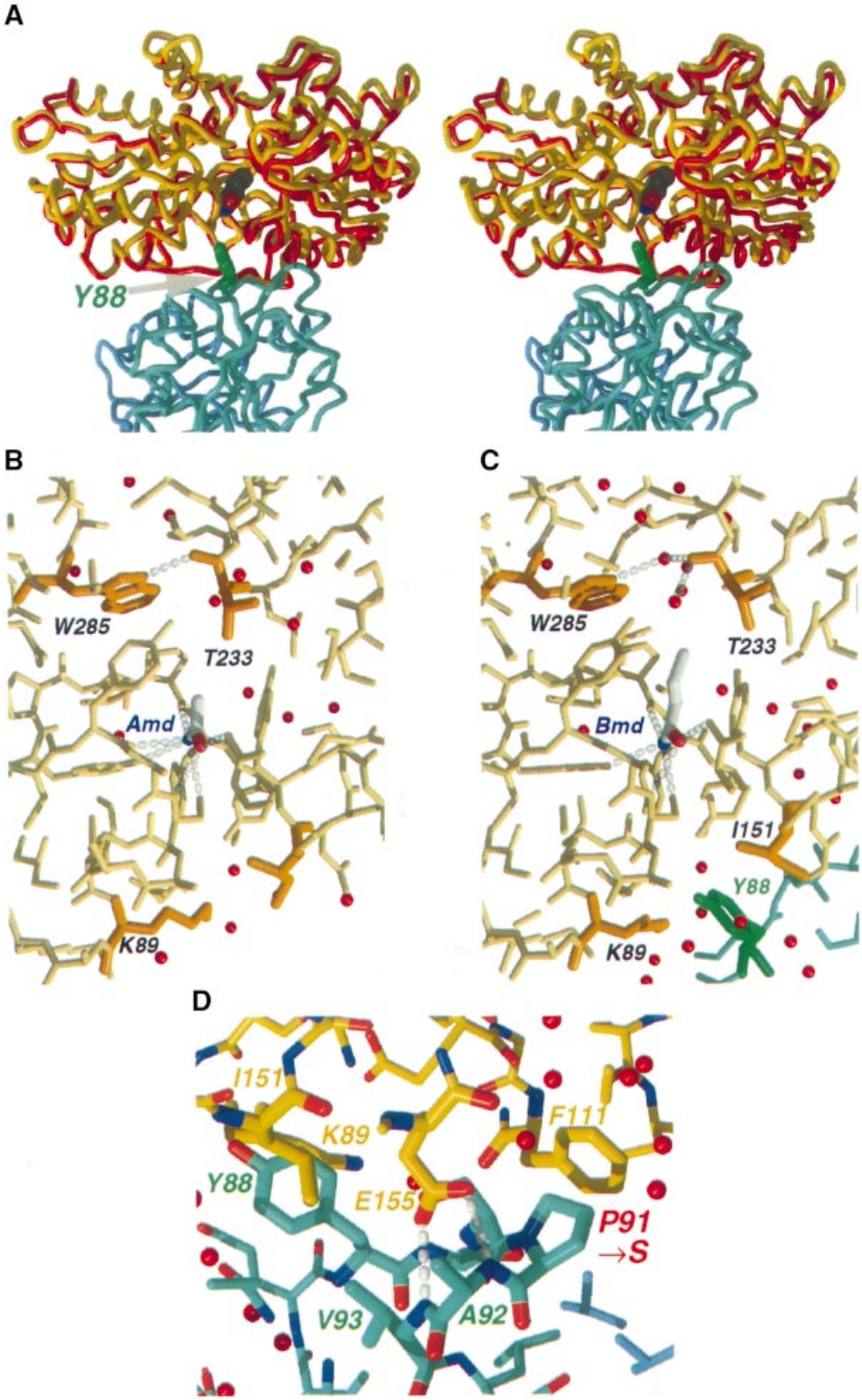

Fig. 5. Mechanism of acetamide induction. (**A**) Stereo-pair showing overlay of 'free' AmiC with bound acetamide (red) on an AmiC molecule in the AmiC–AmiR complex (yellow), with bound butyramide (CPK model). The AmiC molecules were overlaid by superposition of C_α positions from the N-terminal domain (left) only. Y88, which inserts into the mouth of the AmiC interdomain cleft in the AmiC–AmiR complex, is indicated. (**B** and **C**) Details of the AmiC interdomain cleft in the 'free' AmiC structure (B) and the AmiC–AmiR complex (C). Residue pairs K89(C) and I151(C), and T233(C) and W235(C), which make direct contact in the 'free' AmiC structure, are separated by Y88(R) and solvent molecules in the AmiC–AmiR complex. The larger amide-binding pocket, resulting from the relative movement of T233(C) in the AmiC–AmiR complex, accommodates butyramide, which can thus compete with binding of acetamide and act as an 'anti-inducer' or co-repressor *in vivo*. Hydrogen bonding interactions made by the bound butyramide (Bmd) and acetamide (Amd) are shown as broken rods. (**D**) Mutation of Pro91(R) to serine in the mutant strain PAC153 will disrupt the hydrophobic interaction with F111(C), destabilizing the AmiC–AmiR interface so that PAC153 becomes inducible by formamide.

energy contributed by the 1-carbon aliphatic chain of acetamide is sufficient to favour the induced state over the uninduced state. The regulatory genes from PAC153, a formamide-inducible mutant strain (Brammar *et al.*, 1967), have been cloned and sequenced. Despite the change in response to formamide, no mutations were found in the amide-binding site of PAC153–AmiC, consistent with this mutant strain remaining acetamide inducible. However, sequencing of the *amiR* gene from PAC153 revealed a single mutation Pro91→Ser. In the wild-type AmiR, Pro91(R) is an N-terminal helix-cap residue whose Cγ and Cδ side-chain atoms are packed against the face of the side-chain ring of Phe111(C) in AmiC, as part of a the major cluster of interactions between the two proteins in the AmiC–AmiR complex (Figure 5D). Replacement by serine will not disrupt the structure of AmiR, but results in the loss of the favourable hydrophobic interaction between the Pro and Phe side chains at the AmiC–AmiR interface, decreasing the stability of the PAC153 AmiC–AmiR complex relative to wild type. The smaller interaction energy afforded by the binding of formamide rather than acetamide to AmiC is then able to outweigh the decreased stability of this complex, and cause induction of the operon.

The mechanism of transcription antitermination by AmiR

Transcription antitermination provides a powerful mechanism for regulation of the level and/or length of RNA transcripts in bacteria (Rutberg, 1997) and some bacteriophages (DeVito and Das, 1994; Mogridge *et al.*, 1995). However, mechanisms of transcription antitermination vary widely. In the *nus-nut* system of bacteriophage λ (Friedman and Court, 1995), a multiprotein complex of host proteins and a phage protein binds to specific termination sites in nascent RNAs, and modifies RNA polymerase so that it fails to recognize termination signals. A similar mechanism regulates capsule polysaccharide synthesis genes in *E.coli* (Stevens *et al*., 1997). More commonly, transcription antitermination is achieved by the binding of a sequence-specific RNA-binding protein to prevent the formation of terminating stem–loop secondary structures in the nascent mRNA. The best characterized examples of this mechanism are the SacY/BglG family of transcription antiterminators (Rutberg, 1997). These proteins function by stabilizing an alternative stem–loop structure, the ribonucleotide antiterminator or RAT (Aymerich and Steinmetz, 1992), which sequesters the 5′ end of the terminator and prevents its formation. Although structurally unrelated to the receiver-domain response regulators, the SacY/BglG transcription antiterminators are regulated by phosphorylation (Tortosa *et al.*, 1997). A different method for preventing the formation of a transcription terminator, by forming a competing antiterminator in the mRNA, occurs in the regulation of tryptophan biosynthesis genes in *Bacillus subtilis* (Gollnick, 1994). In this system, the more stable antiterminator structure is prevented from forming by the 11-subunit TRAP protein, which binds to (G/U)AG repeats, but only in the presence of tryptophan, thereby allowing formation of the terminator. In the absence of tryptophan, TRAP cannot bind and the antiterminator forms preferentially. The AmiC–AmiR system has significant differences from all of these systems. Thus, unlike the *nus–nut* system, AmiR is polymerase independent, being able to antiterminate transcription by *E.coli*, *P.aeruginosa* or even T7 RNA polymerases (Wilson *et al.*, 1996). Unlike SacY/BglG systems, the ability of AmiR to interact with mRNA is not regulated by phosphorylation, nor does it have any structural similarity to the RNA-binding domains of these proteins (Manival *et al.*, 1997; van Tilbeurgh *et al.*, 1997), and unlike TRAP proteins to which it is also structurally unrelated (Antson *et al.*, 1995), the ligand sensitivity of AmiR is conferred by its interaction with a distinct ligand sensor, and is not an inherent feature.

At the RNA level, the amidase leader sequence is also quite different from those of the TRAP system, in lacking any discernible triplet (or other) repeats. Nor does it possess features resembling the RAT sequences in SacY/BglG systems that could form an alternative stem–loop. Studies of the amidase operon leader mRNA have indicated two regions, CCGAAC and CACAGAGCA, starting 36 and 54 bases, respectively, downstream of the start of transcription, in which point mutations abolish transcription antitermination by AmiR (Wilson *et al.*, 1996). The 12 bases between these sites are insensitive to missense mutations, but insertions or deletions into this intervening segment lower transcription antitermination efficiency, suggesting that the three-dimensional presentation of these two regions is important in efficient interaction with AmiR.

By analogy with classical two-domain response regulators, the RNA-binding ‘effector’ function of AmiR should reside in the C-terminal region of the protein, and this is confirmed by truncation mutants (Δ179–195, Δ162–195) where loss of C-terminal residues abolishes antitermination activity (Table I). However, if these regions are sufficient for specific RNA binding and antitermination, it is not clear why AmiC molecules bound to the N-terminal domains should block that activity, as the C-termini are fully accessible in the AmiC–AmiR complex (Figure 4). The N-terminal domains, whose accessibility changes dramatically on release of AmiC, appear to play no direct role in RNA binding or antitermination. Thus, mutations on the AmiC-binding surface of AmiR (Pro91Ser, Tyr88Ala) change the sensitivity of induction, but have no effect on the ability of the mutant AmiR to antiterminate (Table I). The assumption that the structural state of AmiR observed in the AmiC–AmiR complex is that which binds to RNA may be naive. AmiR might undergo some significant change in conformation or oligomerization state on release from AmiC, which converts it to an ‘active’ form. However, the nature of such a change is not at all obvious. Dissociation to monomers is very unlikely, as there is an extensive hydrophobic interface throughout the AmiR dimer, whose disruption would be very unfavourable. Reorganization of the C-terminal segments into a globular conformation similar to the C-terminal domains of DNA-binding response regulators, such as NarL, is also very unlikely as this would disrupt the favourable coiled-coil interface between the two monomers, and in any event, would not be prevented by the presence of the AmiC molecules in the complex.

The solution to this paradox lies in the behaviour of the AmiR protein on release from the AmiC–AmiR complex upon addition of acetamide *in vitro*. In size-exclusion chromatography, AmiC–AmiR migrates as a

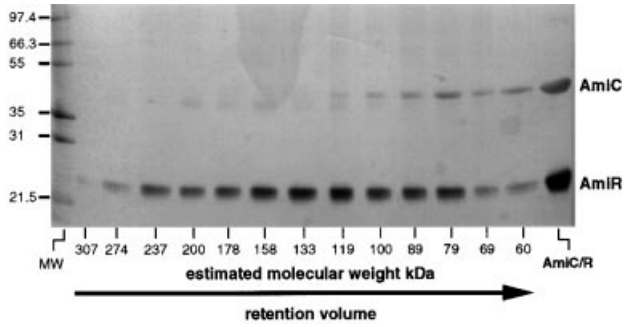

Fig. 6. Oligomerization of AmiR on release from AmiC–R. Silver-stained SDS–PAGE gel showing elution of free AmiR and free AmiC from a size-exclusion column, calibrated using molecular weight standards. Intact AmiC–R complex (~16 mg/ml in 20 mM Tris pH 9.0, 150 mM NaCl, 1 mM EDTA, 1 mM DTT, 3.4 mM butyramide) was injected on to a Superose 12 10/30 column (Pharmacia), pre-equilibrated and developed with buffer containing 20 mM Tris pH 9.0, 600 mM NaCl, 1 mM EDTA, 1 mM DTT, 50 mM acetamide. The >10-fold excess of acetamide causes complete dissociation of the AmiC–R complex under these conditions. AmiR elutes after the void volume of the column, but at retention volumes corresponding to molecular weights in the range 100–200 kDa. AmiC elutes later than the majority of AmiR, in a molecular weight range consistent with dimers and monomers, as previously observed (Chamberlain *et al.*, 1997). AmiR shows anomalously strong staining by silver relative to AmiC, as can be seen from the right-hand lane, in which intact AmiC–AmiR complex (1:1 molar stoichiometry) is loaded.

single species with an estimated molecular weight of ~130 kDa, consistent with a composition of 2 × AmiC + 2 × AmiR (Wilson *et al.*, 1996). When AmiC–AmiR is injected into a gel filtration column equilibrated with an excess of acetamide, free AmiC is observed eluting later than would the AmiC–AmiR complex, consistent with a dimer of ~85 kDa and a monomer of ~43 kDa. Surprisingly, no late-running AmiR corresponding to the ~45 kDa free dimer or ~23 kDa monomer is observed. Instead, only fast-running AmiR species are observed, eluting well after the void but ahead of the AmiC, with estimated molecular weight in the range 100–200 kDa (Figure 6). This molecular weight range would be consistent with oligomers containing between four and eight AmiR molecules. Thus, on release from the AmiC–AmiR complex, AmiR does indeed undergo a change of state, associating into a high-molecular-weight form which is competent in sequence-specific RNA binding. The role of AmiC is therefore not simply that of an inhibitor of AmiR, but rather that of a ligand-regulated molecular chaperone, holding AmiR in a state where it cannot associate into a multimeric antitermination complex until the appropriate time. The stoichiometry and structure of this higher-molecular-weight form of AmiR, and the structural basis for its sequence-specific interaction with RNA, remain to be determined.

Materials and methods

Cloning and mutagenesis

Plasmids pRAN1 and pRAN153 carry the PCR-amplified *amiC* and *amiR* genes from wild-type strain PAC1 (Kelly and Clarke, 1962) and the formamide-inducible strain PAC153 (Brammar *et al.*, 1967), respectively, in the vector pMMB66EH. The construction and characterization of pRAN1 and pRAN153 are described fully in R.A.Norman, B.P.O'Hara, L.H.Pearl and R.E.Drew (manuscript in preparation). For mutagenesis, the *amiC* and *amiR* genes, including the 20 bp upstream of the *amiC* translational start site, were cloned by PCR from plasmid pAS20 (Wilson and Drew, 1991), and the resulting 1.8 kb fragment cloned into *Kpn*I/*Xba*I cleaved pBluescript II KS (Stratagene, La Jolla, CA) and designated pBSKCR. Mutagenesis was accomplished using the Quickchange™ Site-Directed Mutagenesis Kit (Stratagene, La Jolla, CA) using pBSKCR as the parental template. Mutants were confirmed by ABI sequencing.

Table II. Crystallographic statistics

Data collection	All data (outer shell)
R_{merge}	6.9 (20.2)
I/σ (I)	6.8 (3.0)
Completeness (%)	83.8 (69.3)
Multiplicity	2.7 (1.50)
No. of unique reflections	60 571 (7252)
Structure refinement	
No. of atoms (protein)	8802
No. of atoms (all)	9662
Resolution range (Å)	20.0–2.25
R_{cryst}	0.186
R_{free}	0.256

Transcription antitermination activity of amiC–R constructs

Transcription antitermination activity and amide sensitivity of *amiC–R* were determined *in vivo* in *E.coli*, using pBSKCR expressing wild-type *amiC* and wild-type or mutant *amiR*. Activity was measured by amidase assay with the cognate amidase gene (*amiE*) present on a second plasmid as previously described (Wilson *et al.*, 1993), and also by β-galactosidase assay (Miller, 1972). In the latter case, the leader sequence of the amidase operon was cloned upstream of the *E.coli* β-galactosidase structural gene (*lac*Z) into the chromosomal insertion vector Mini-TnKn (de Lorenzo *et al.*, 1990). A single chromosomal insertion of the *ami*E leader sequence (nucleotides 1–262)::*lac*Z fusion in the *E.coli* strain XL-1 Blue (Stratagene, La Jolla, CA) was isolated and designated XL Int. All β-galactosidase assays were conducted with this strain (R.A.Norman, B.P.O'Hara, L.H.Pearl and R.E.Drew, manuscript in preparation).

Expression, purification and crystallization of the AmiC–AmiR–butyramide complex

The AmiC–AmiR–butyramide complex was purified from *P.aeruginosa* PAC452, pRAN1 as described (R.A.Norman, B.P.O'Hara, L.H.Pearl and R.E.Drew, manuscript in preparation). The complex, essentially free of contaminants, was concentrated to 16 mg/ml in 20 mM Tris pH 9.0, 150 mM NaCl, 1 mM EDTA, 1 mM dithiothreitol (DTT), 34 mM butyramide. Large single crystals suitable for diffraction studies were grown using a combination of micro-batch crystallization under mineral oil (Chayen *et al.*, 1992) and streak seeding (Stura and Wilson, 1991). Optimal crystallization conditions were found to be: polyethylene glycol 4000 (8–8.5% w/v) and propan-2-ol (20% v/v), buffered with sodium citrate (50 mM, pH 5.6), and AmiC–AmiR complex present at 5 mg/ml (final concentration). The crystallization buffer with 20% (v/v) glycerol in place of propan-2-ol was used both as a recovery and cryoprotection solution.

Data collection, structure determination and refinement

Diffraction data to 2.25 Å were obtained from a single plate crystal of approximate dimensions 0.6 × 0.2 × 0.05 mm. Data were collected at 100 K on beam line 7.2 (λ = 1.448 Å) at the Synchrotron Radiation Source, CLRC Daresbury Laboratory, on a MAR 345 Image Plate Detector. The AmiC–AmiR complex crystallizes in space group C2 with unit cell dimensions a = 308.44 Å, b = 67.15 Å, c = 76.41 Å and β = 103.33°. Diffraction images were integrated using MOSFLM (Leslie, 1995), and merged and reduced using SCALA and other programs of the CCP4 program suite (CCP4, 1994). Statistics for the data collection are given in Table II.

Initial phases were determined by molecular replacement with the refined structure of AmiC (PDB Code: 1PEA) using AMoRe (Navaza, 1994). Two independent solutions were obtained, which were approximately related by a non-crystallographic diad evident in self-rotation functions. Phases were improved by positional refinement against a maximum-likelihood residual using REFMAC (Murshudov *et al.*, 1997) and ARP (Lamzin and Wilson, 1997) to give a map in which the AmiR dimer could be identified. Alternating cycles of manual intervention

using 'O' (Jones *et al.*, 1991) and automated refinement using REFMAC gave the final model. Statistics for the refinement are given in Table 2. All molecular graphics images were generated using Robert Esnouf's adaptation of MOLSCRIPT (Kraulis, 1991) and RASTER3D (Merrit and Murphy, 1994), except for Figures 2C and 4A,B, which were created with GRASP (Nicholls *et al.*, 1993).

Acknowledgements

We thank John Ladbury for useful discussions, Frances Pearl and Christine Orengo for assistance with database searches, and Simon Wachira and Stuart Wilson for their considerable contributions at earlier stages. We are grateful to the Ludwig Institute for Cancer Research and the CLRC Daresbury Laboratory for X-ray diffraction facilities. This work has been supported by project grants from the Wellcome Trust and BBSRC to R.E.D. and L.H.P. R.A.N. acknowledges the receipt of a BBSRC Research Studentship; T.E.B. is a BBSRC David Phillips Research Fellow.

References

Antson,A.A. *et al.* (1995) The structure of Trp RNA-binding attenuation protein. *Nature*, **374**, 693–700.

Aymerich,S. and Steinmetz,M. (1992) Specificity determinants and structural features in the RNA target of the bacterial antiterminator proteins of the BglG/SacY family. *Proc. Natl Acad. Sci. USA*, **89**, 10410–10414.

Baikalov,I., Schroeder,I., Kaczor-Grzeskowiak,M., Grzeskowiak,K., Gunsalus,R. and Dickerson,R.E. (1996) Structure of the *Escherichia coli* response regulator NarL. *Biochemistry*, **35**, 11035–11061.

Barak,R. and Eisenbach,M. (1992) Correlation between phosphorylation of the chemotaxis protein CheY and its activity at the flagellar motor. *Biochemistry*, **31**, 1821–1826.

Brammar,W.J., Clarke,P.H. and Skinner,A.J. (1967) Biochemical and genetic studies with regulator mutants of the *Pseudomonas aeruginosa* 8602 amidase system. *J. Gen. Microbiol.*, **47**, 87–102.

CCP4 (1994) Programs for protein crystallography. *Acta Crystallogr. D*, **50**, 760–763.

Chamberlain,D., Ohara,B.P., Wilson,S.A., Pearl,L.H. and Perkins,S.J. (1997) Oligomerization of the amide sensor protein AmiC by X-ray and neutron scattering and molecular modeling. *Biochemistry*, **36**, 8020–8029.

Chayen,N.E., Stewart,P.D.S. and Blow,D.M. (1992) Microbatch crystallization under oil—a new technique allowing many small-volume crystallization trials. *J. Cryst. Growth*, **122**, 176–180.

Cousens,D.J., Clarke,P.H. and Drew,R. (1987) The amidase regulatory gene (*amiR*) of *Pseudomonas aeruginosa*. *J. Gen. Microbiol.*, **133**, 2041–2052.

DeVito,J. and Das,A. (1994) Control of transition processivity in phage λ: Nus factors strengthen the termination-resistant state of RNA polymerase induced by N terminator. *Proc. Natl Acad. Sci. USA*, **91**, 8660–8664.

Djordjevic,S., Goudreau,P.N., Xu,Q., Stock,A.M. and West,A.H. (1998) Structural basis for methylesterase CheB regulation by a phosphorylation-activated domain. *Proc. Natl Acad. Sci. USA*, **95**, 1381–1386.

Drew,R. and Lowe,N. (1989) Positive control of *Pseudomonas aeruginosa* amidase synthesis is mediated by a transcription anti-termination mechanism. *J. Gen. Microbiol.*, **135**, 817–823.

Friedman,D.I. and Court,D.L. (1995) Transcription antitermination: the λ paradigm updated. *Mol. Microbiol.*, **18**, 191–200.

Ganguli,S., Wang,H., Matsumura,P. and Volz,K. (1995) Uncoupled phosphorylation and activation in bacterial chemotaxis–the 2.1 Å structure of a threonine to isoleucine mutant at position-87 of CheY. *J. Biol. Chem.*, **270**, 17386–17393.

Gollnick,P. (1994) Regulation of the *Bacillus subtilis trp* operon by an RNA-binding protein. *Mol. Microbiol.*, **11**, 991–997.

Gutierrez,J.-C., Ramos,F., Ortner,L. and Tortolero,M. (1995) nasST, two genes involved in the induction of the assimilatory nitrite-nitrate reductase operon (nasAB) of *Azotobacter vinelandii*. *Mol. Microbiol.*, **18**, 579–591.

Hakenbeck,R. and Stock,J.B. (1996) Analysis of two-component signal transduction systems involved in transcriptional regulation. *Methods Enzymol.*, **273**, 281–300.

Harrison,S.C. (1991) A structural taxonomy of DNA-binding domains. *Nature*, **353**, 715–719.

Hess,J.F., Bourret,R.B. and Simon,M.I. (1988) Histidine phosphorylation and phosphoryl group transfer in bacterial chemotaxis. *Nature*, **336**, 139–143.

Imamura,A., Hanaki,N., Umeda,H., Nakamura,A., Suzuki,T., Ueguchi,C. and Mizuno,T. (1998) Response regulators implicated in His-to-Asp phosphotransfer signaling in *Arabidopsis*. *Proc. Natl Acad. Sci. USA*, **95**, 2691–2696.

Jones,T.A., Zou,J.-Y., Cowan,S.W. and Kjeldgaard,M. (1991) Improved methods for building protein models in electron density maps and the location of errors in these models. *Acta Crystallogr. A*, **47**, 110–119.

Kelly,M. and Clarke,P.A. (1962) An inducible amidase produced by a strain of *Pseudomonas aeruginosa*. *J. Gen. Microbiol.*, **27**, 305–316.

Kraulis,P.J. (1991) MOLSCRIPT—A program to produce both detailed and schematic plots of protein structures. *J. Appl. Crystallogr.*, **24**, 946–950.

Lamzin,V.S. and Wilson,K.S. (1997) Automated refinement for protein crystallography. *Methods Enzymol.*, **277**, 269–305.

Leslie,A.G.W. (1995) *MOSFLM Users Guide*. MRC Laboratory of Molecular Biology, Cambridge, UK

Lewis,M., Chang,G., Horton,N.C., Kercher,M.A., Pace,H.C., Schumacher,M.A., Brennan,R.G. and Lu,P.Z. (1996) Crystal structure of the lactose operon repressor and its complexes with DNA and inducer. *Science*, **271**, 1247–1254.

De Lorenzo,V., Herrero,M., Jakubzil,U. and Timmis,K.N. (1990) Mini-Tn5 transposon derivatives for insertion mutagenesis, promoter probing and chromosomal insertion of cloned DNA in Gram-negative eubacteria. *J. Bacteriol.*, **172**, 6568–6572.

Lukat,G.S., Lee,B.H., Mottonen,J.M., Stock,A.M. and Stock,J.B. (1991) Roles of the highly conserved aspartate and lysine residues in the response regulator of bacterial chemotaxis. *J. Biol. Chem.*, **266**, 8348–8354.

Madhusudan, Zapf,J., Whiteley,J.M., Hoch,J.A., Xuong,N.H. and Varughese,K.I. (1996) Crystal structure of a phosphatase-resistant mutant of sporulation response regulator Spo0F from *Bacillus subtilis*. *Structure*, **4**, 679–690.

Manival,X., Yang,Y., Strub,M.P., Kochoyan,M., Steinmetz,M. and Aymerich,S. (1997) From genetic to structural characterization of a new class of RNA-binding domain within the SacY/BglG family of antiterminator proteins. *EMBO J.*, **16**, 5019–5029.

Martinez-Hackert,E. and Stock,A.M. (1997) The DNA-binding domain of OmpR: crystal structure of a winged helix trancription factor. *Structure*, **5**, 109–124.

Merrit,E.A. and Murphy,M.E.P. (1994) Raster3D version 2.0—a program for photorealistic molecular graphics. *Acta Crystallogr. D*, **50**, 869–873.

Miller,J.H. (1972) *Experiments in Molecular Genetics*. Cold Spring Harbor Laboratory Press, Cold Spring Harbor, NY.

Mogridge,J., Mah,T.-F. and Greenblatt,J. (1995) A protein–RNA interaction network facilitates the template-independent cooperative assembly on RNA polymerase of a stable antitermination complex containing the λ N protein. *Genes Dev.*, **9**, 2831–2841.

Murshudov,G.N., Vagin,A.A. and Dodson,E.J. (1997) Refinement of macromolecular structures by the maximum-likelihood method. *Acta Crystallogr. D*, **53**, 240–255.

Navaza,J. (1994) AMoRE—an automated package for molecular replacement. *Acta Crystallogr. A*, **50**, 157–163.

Nicholls,A., Bharadwaj,R. and Honig,B. (1993) GRASP—graphical representation and analysis of surface properties. *Biophys. J.*, **64**, A116.

Parkinson,J.S. (1993) Signal transduction schemes of bacteria. *Cell*, **73**, 857–871.

Pearl,L.H., O'Hara,B.P., Drew,R.E. and Wilson,S.A. (1994) Crystal structure of AmiC—the controller of transcription antitermination in the amidase operon of *Pseudomonas aeruginosa*. *EMBO J.*, **13**, 5810–5817.

Quiocho,F.A. (1991) Atomic structures and function of periplasmic receptors for active transport and chemotaxis. *Curr. Opin. Struct. Biol.*, **1**, 922–933.

Roman,S.J., Meyers,M., Volz,K. and Matsumura,P. (1992) A chemotactic signalling surface on CheY defined by suppressors of flagellar motor mutations. *J. Bacteriol.*, **171**, 3609–3618.

Rutberg,B. (1997) Antitermination of transcription of catabolic operons. *Mol. Microbiol.*, **23**, 413–421.

Sanders,D.A., Gillece-Castro,B.L., Stock,A.M., Burlingame,A.L. and Koshland,D.E.,Jr. (1989) Identification of the site of phosphorylation of the chemotaxis response regulator protein CheY. *J. Biol. Chem.*, **264**, 21770–21778.

Sanders,D.A., Gillece,C.B., Burlingame,A.L. and Koshland,D.E.,Jr. (1992) Phosphorylation site of NtrC, a protein phosphatase whose covalent intermediate activates transcription. *J. Bacteriol.*, **174**, 5117–5122.

Stevens,M.P., Clarke,B.R. and Roberts,I.S. (1997) Regulation of the *Escherichia coli* K5 capsule gene cluster by transcription antitermination. *Mol. Microbiol.*, **24**, 1001–1012.

Stock,A.M., Mottonen,J.M., Stock,J.B. and Schutt,C.E. (1989) Three-dimensional structure of CheY, the response regulator of bacterial chemotaxis. *Nature*, **337**, 745–749.

Stock,J.B., Stock,A.M. and Mottonen,J.M. (1990) Signal transduction in bacteria. *Nature*, **344**, 395–400.

Stock,A.M., Martinez-Hackert,E., Rasmussen,B.F., West,A.H., Stock,J.B., Ringe,D. and Petsko,G.A. (1993) Structure of the Mg^{2+}-bound form of CheY and mechanism of phosphoryl transfer in bacterial chemotaxis. *Biochemistry*, **32**, 13375–13380.

Stura,E.A. and Wilson,I.A. (1991) Applications of the streak seeding technique in protein crystallization. *J. Cryst. Growth*, **110**, 270–282.

Thomason,P.A., Traynor,D., Cavet,G., Chang,W.-T., Harwood,A.J. and Kay,R.R. (1998) An intersection of the cAMP/PKA and two-component signal transduction systems in *Dictyostelium*. *EMBO J.*, **17**, 2838–2845.

Tortosa,P., Aymerich,S., Lindner,C., Saier,M.H., Reizer,J. and Le Coq,D. (1997) Multiple phosphorylation of SacY, a *Bacillus subtilis* transcriptional antiterminator negatively controlled by the phosphotransferase system. *J. Biol. Chem.*, **272**, 17230–17237.

van Tilbeurgh,H., Manival,X., Aymerich,S., Lhoste,J.-M., Dumas,C. and Kochoyan,M. (1997) Crystal structure of a new RNA-binding domain from the antiterminator protein SacY of *Bacillus subtilis*. *EMBO J.*, **16**, 5030–5036.

Volz,K. (1993) Structural conservation in the CheY superfamily. *Biochemistry*, **32**, 11741–11753.

Volz,K. and Matsumura,P. (1991) Crystal structure of *Escherichia coli* CheY refined at 1.7 Å resolution. *J. Biol. Chem.*, **266**, 15511–15519.

Wilson,S. and Drew,R. (1991) Cloning and DNA sequence of amiC, a new gene regulating expression of the *Pseudomonas aeruginosa* aliphatic amidase and purification of the AmiC product. *J. Bacteriol.*, **173**, 4914–4921.

Wilson,S.A. and Drew,R.E. (1995) Transcriptional analysis of the amidase operon from *Pseudomonas aeruginosa*. *J. Bacteriol.*, **177**, 3052–3057.

Wilson,S.A., Wachira,S.J., Drew,R.E., Jones,D. and Pearl,L.H. (1993) Antitermination of amidase expression in *Pseudomonas aeruginosa* is controlled by a novel cytoplasmic amide-binding protein. *EMBO J.*, **12**, 3637–3642.

Wilson,S.A., Wachira,S.J.M., Norman,R.A., Pearl,L.H. and Drew,R.E. (1996) Transcription antitermination regulation of the *Pseudomonas aeruginosa* amidase operon. *EMBO J.*, **15**, 5907–5916.

Received June 15, 1999; revised and accepted August 6, 1999